# HIGH ACCURACY ISENTROPIC COMPRESSION STUDIES WITH HIGH EXPLOSIVE PULSED POWER *

**D.G. Tasker[ξ], J.H. Goforth, H. Oona**
*Los Alamos National Laboratory, DE-6, MS J566*
*Los Alamos, NM 87545, USA*

*Abstract*

An study of the one-dimensional isentropic compression experiment (ICE), performed with High Explosive Pulsed Power (HEPP), has demonstrated that accurate, high stress, isentropic Equations of State (EOS) data may be obtained with this technique.

The physics and accuracy of electromagnetic loading in the ICE technique is presented. It is shown that the HEPP-ICE load configuration is capable of producing magnetic stresses that are uniform to 1 part in 1000 over the central 87% of the sample faces, and that HEPP-ICE provides exact matching of the stresses between opposing samples. This magnetic uniformity, the exact matching, and the large sample samples possible with HEPP-ICE, are necessary for the highest accuracy isentropic EOS data.

Isentropic EOS data have been obtained with a prototype HEPP-ICE system, and the results for tungsten and copper demonstrate the inaccuracy of the technique, which may be as low as 0.2% in stress. It is shown that a large-scale HEPP-ICE system is capable of producing shock-free loading up to 2.2 TPa in 10-mm thick tungsten samples.

## I. INTRODUCTION

The basic techniques of HEPP-ICE have been described previously [1,2,3]. The original ICE technique is due to Asay [4], and a significant body of ICE work has been conducted on the Z-machine at the Sandia National Laboratory. In the ICE experiment, smoothly rising (shock-free) mechanical compression waves are propagated into matched samples of different thicknesses by electromagnetic loading in a planar geometry. A complete EOS isentrope is acquired in one experiment, i.e., continuously from zero up to the peak stress. Good quality isentropic EOS data have been obtained for many materials [5,6,7].

### *A. ICE method*

Two identical samples, with a difference in thickness of $h$, are compressed by *identical* B-forces and their particle velocity profiles, $u(t)$, are obtained from VISAR measurements at the rear free surfaces, Figure 1. The magnetic stress is given by the vector cross-product $P_B = J \times B$, where $J$ is the current per unit width ($dI/dW$). In the simplest case, when the plate width, $W >> d$, the plate separation, the magnetic field on the inside surface of one conductor due the current in the opposing surface is $\frac{1}{2}\mu_0 J$ (SI units are used throughout this paper). Then the stress normal to the inside surfaces $P_B = J \times B = \frac{1}{2}\mu_0 J^2$. (As $d$ increases with time and/or when the current is non-steady, then $B < \frac{1}{2}\mu_0 J^2$ and becomes non-uniform, see below.)

Using Lagrangian wave analysis [8] the Lagrangian wave speed is $C_L(u) = h \div \Delta t$. The differential form of the Lagrangian momentum conservation equation is

$$d\sigma = \rho_0 c_L(u) du \qquad (1)$$

which is used to calculate the change in stress, $d\sigma$, for each change (step) in particle velocity, $du$, going up the curve $u(t)$, where $\rho_0$ is the initial density ($h$ and $\rho_0$ are constant in Lagrangian space). Continuous EOS

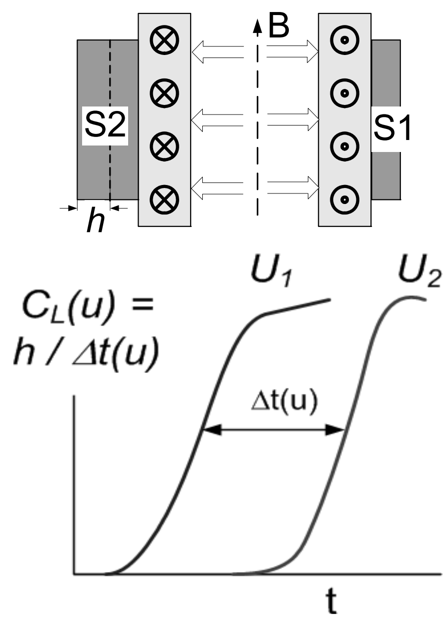


**Figure 1.** Top: Velocities $U_1$ and $U_2$ are measured at the outer surfaces of samples S1, S2. Bottom: velocity $C_L(u)$ is obtained from $U_1$ and $U_2$, point by point.

* Work supported by US Department of Energy, LA-UR-07-3893
ξ email:tasker@lanl.gov

# Report Documentation Page

*Form Approved*
*OMB No. 0704-0188*



| 1. REPORT DATE | 2. REPORT TYPE | 3. DATES COVERED |
|---|---|---|
| **JUN 2007** | **N/A** | **-** |

| 4. TITLE AND SUBTITLE | |
|---|---|
| **High Accuracy Isentropic Compression Studies With High Explosive Pulsed Power** | 5a. CONTRACT NUMBER |
| | 5b. GRANT NUMBER |
| | 5c. PROGRAM ELEMENT NUMBER |
| 6. AUTHOR(S) | 5d. PROJECT NUMBER |
| | 5e. TASK NUMBER |
| | 5f. WORK UNIT NUMBER |
| 7. PERFORMING ORGANIZATION NAME(S) AND ADDRESS(ES) **Los Alamos National Laboratory, DE-6, MS J566 Los Alamos, NM 87545, USA** | 8. PERFORMING ORGANIZATION REPORT NUMBER |
| 9. SPONSORING/MONITORING AGENCY NAME(S) AND ADDRESS(ES) | 10. SPONSOR/MONITOR'S ACRONYM(S) |
| | 11. SPONSOR/MONITOR'S REPORT NUMBER(S) |

12. DISTRIBUTION/AVAILABILITY STATEMENT

**Approved for public release, distribution unlimited**

13. SUPPLEMENTARY NOTES

**See also ADM002371. 2013 IEEE Pulsed Power Conference, Digest of Technical Papers 1976-2013, and Abstracts of the 2013 IEEE International Conference on Plasma Science. IEEE International Pulsed Power Conference (19th). Held in San Francisco, CA on 16-21 June 2013.**

14. ABSTRACT

**An study of the one-dimensional isentropic compression experiment (ICE), performed with High Explosive Pulsed Power (HEPP), has demonstrated that accurate, high stress, isentropic Equations of State (EOS) data may be obtained with this technique. The physics and accuracy of electromagnetic loading in the ICE technique is presented. It is shown that the HEPP-ICE load configuration is capable of producing magnetic stresses that are uniform to 1 part in 1000 over the central 87% of the sample faces, and that HEPP-ICE provides exact matching of the stresses between opposing samples. This magnetic uniformity, the exact matching, and the large sample samples possible with HEPP-ICE, are necessary for the highest accuracy isentropic EOS data. Isentropic EOS data have been obtained with a prototype HEPP-ICE system, and the results for tungsten and copper demonstrate the inaccuracy of the technique, which may be as low as 0.2% in stress. It is shown that a large-scale HEPP-ICE system is capable of producing shock-free loading up to 2.2 TPa in 10-mm thick tungsten samples.**

15. SUBJECT TERMS

| 16. SECURITY CLASSIFICATION OF: | | | 17. LIMITATION OF ABSTRACT | 18. NUMBER OF PAGES | 19a. NAME OF RESPONSIBLE PERSON |
|---|---|---|---|---|---|
| a. REPORT | b. ABSTRACT | c. THIS PAGE | | | |
| **unclassified** | **unclassified** | **unclassified** | **SAR** | **4** | |

relationships between stress, wave speed, particle velocity, etc., from zero to the peak stress are thus obtained.

### *B. HEPP-ICE apparatus*

A 6 mF, 20 kV capacitor bank provides a seed current of ~2 MA to a 4-in×5-in plate flux compressor [2]. The FCG transfers up to 12 MA into a storage inductor of ~25 nH and an explosively-formed fuse (EFF) opening switch. Three parallel explosively-driven polyimide closing switches [9] then transfer current to the load at the appropriate time. This prototype circuit is capable of delivering 7 MA (dI/dt ~3 $\times 10^{13}$ A/s) into loads of typically 1 to 2 cm width and will produce isentropic compression at stresses in the range of 0 to 250 GPa. However, advanced HEPP-ICE systems are capable of producing isentropic data beyond 2 TPa [10].

### *C. Stress uniformity and exact B-field matching in an HEPP-ICE load*

It is crucial that the samples are subjected to *identical* and *uniform* magnetic stresses. Previously we showed that for static current flow the B-field becomes increasing non-uniform across the width as the ratio of separation to width, *d/W*, is increased [11]. However, during the EOS-data gathering portions of ICE experiments the current is always rising in the load, i.e., $dI/dt > 0$. The rise is approximately sinusoidal, rising from 0 to π/2 over ~½μs. For parallel plates, the current flows preferentially along the outside edges of the load, where the specific electrical impedance is a minimum. The dynamic current and stress distributions have been modeled with a finite element partial differential equation code [12]; the stress plot is shown in Figure 2.

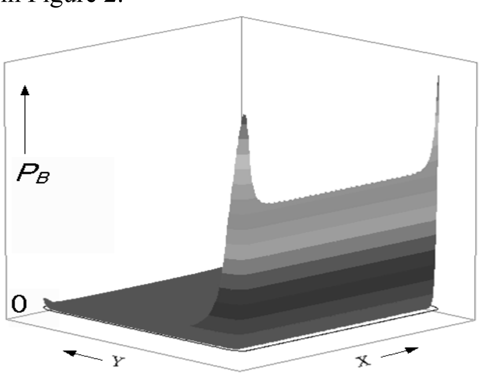


**Figure 2**. Magnetic stress $P_B$ on the inside surface of a parallel conductor. The width of the conductor is along the *X*-axis, the thickness along the *Y*-axis (drawn to a 4x larger scale than the X axis for clarity).

The calculation shows that for the parallel plate configuration used in HEPP-ICE, under typical dynamic conditions, the stress is uniform to 1 part in $10^3$ across the central 87% of the conductors. (The plot is for a *d/W* ratio of 0.3, which would occur towards the end of experiment, when uniformity is at its worst.)

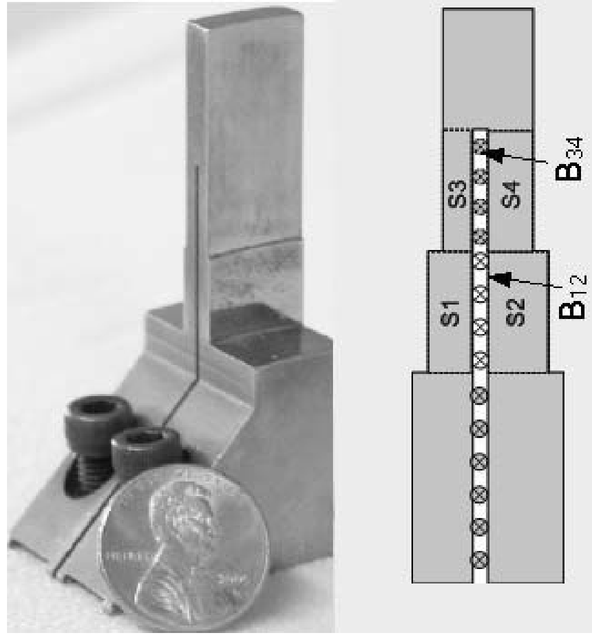


**Figure 3.** Left: the HEPP-ICE load. Right: the four samples, S1 to S4; the magnetic fields (⊗) common to samples S1&S2, $B_{12}$; and the corresponding field for S3&S4, $B_{34}$.

For exactly matched magnetic stress loading, the sample positions are important. In Figure 3 two opposing sample pairs, S1 and S2, S3 and S4 are shown and they share the magnetic fields $B_{12}$ and $B_{34}$. Currents flow in and out from the source at the bottom, and as they do so, the currents redistribute themselves as the samples separate under magnetic loading. The samples will have different thicknesses and may have different acoustic impedances and will consequent separate with different accelerations. We have found that the stresses corresponding to $B_{12}$ and $B_{34}$ may differ by as much as 5%. The advantages of the parallel plate configuration used in HEPP-ICE are that the B-fields and stresses are *exactly* matched for opposing samples because they always share the *same* B-field and the central B-field is very uniform.

### *D. Higher stresses, larger sample sizes and higher accuracy in HEPP-ICE experiments*

One important advantage of the HEPP-ICE over other ICE techniques is that the experiment can be scaled to any magnitude of current, and hence stress, by simply by choosing the appropriate HEPP components. When designing an ICE experiment it is important to prevent the ramp wave developing into a shock wave by the so-called shock-up process. Shock-up is caused by the fact that the compression wave velocity is stress dependent, and in most materials the wave velocity increases with stress. Should shock-up occur in any of the samples in an HEPP-ICE experiment, the compression of the material would no longer be isentropic after the shock has developed. The maximum stress and sample size ultimately depend on how well the shock-up in a material can be delayed. The method of characteristics [13] can be used to design the optimum current profiles to prevent shock-up, they are shown for 2.2-TPa HEPP-ICE experiments and 20-mm wide tungsten samples in Figure 4. Here, the maximum thickness without shock-up is 10 mm, the maximum current is 65 MA, and the risetime is 2 µs. The current, peak *dI/dt* (40 TA/s) and risetime are well within the capabilities of existing HEPP components presently used at LANL.

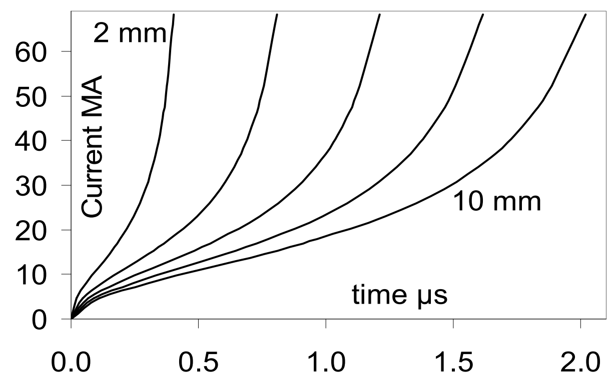


**Figure 4**. Ideal current waveforms for shock-free ICE measurements up to 2.2 TPa. The sample thicknesses are 2, 4, 6, 8 and 10 mm.

HEPP-ICE is the only technique capable of providing such long current waveforms, and therefore the only technique capable of producing shock-free conditions at these large stresses and in such large samples. One obvious advantage of these large sample sizes is that the relative errors in thickness and time measurement are reduced, see section III.

## II. HEPP-ICE EOS RESULTS

The LANL HEPP-ICE program has focused on developing the HEPP techniques to produce high stress EOS data, and relatively few data gathering experiments have been performed. The data for OFHC copper were presented previously [3]. Here we will present the data for pure tungsten. There are two techniques we use for data analysis, the generalized Lagrangian approach described in the Introduction, and the Backward technique [14]. Due to space limitations, only the results of the generalized technique are shown.

The results for copper showed that the HEPP-ICE is capable of resolving differences between isentropes as small as 0.2%. These EOS data for pure tungsten were obtained from a series experiments were the sample thicknesses ranged from 1 to 4 mm. The pressure vs. particle velocity ($P$, $u$) isentropes were obtained by fitting quadratics to the stress vs. $u$ data above the elastic-plastic transition, then setting the constant term to zero so that the data intersected the origin; see Figure 5 which shows the data and the calculated isentrope. The data agree to within 1%, which is also the estimated error in these tungsten experiments caused by the difficulties of measuring the sample thicknesses to the required accuracy in this particular experiment.

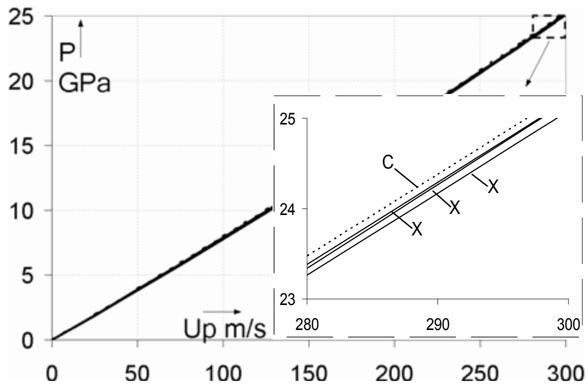


**Figure 5**. Tungsten: pressure vs. particle velocity data. Within the inset, X = HEPP-ICE data, C = calculated isentrope.

## III. ACCURACY OF ICE TECHNIQUE

The accuracy of the ICE technique is limited by the accuracy of the wave and particle velocity measurements, and the uniformity of the stress loading. Substituting *Δ's* for the *d*'s in Equation (1) to represent the finite steps in the data, the fractional error of steps in stress is

$$\frac{d\Delta\sigma}{\Delta\sigma} \approx \frac{dh}{h} + \frac{d\Delta u}{\Delta u} + c_L(u)\frac{d\Delta t}{h} \qquad (2)$$

where the three terms on the right hand side are the fractional errors in thickness, particle velocity and transit time. Note that the transit time is $\Delta t = h \div C_L(u)$, so the timing error increases with wave velocity $C_L(u)$.

The inaccuracy of the VISAR surface velocity measurement can be as small as 0.1% with careful preparation, and may be ~2% otherwise [15]. The measurement of wave velocity is $C_L(u) = h \div \Delta t$, and both $h$ (thickness) and $\Delta t$ (time difference) are sources of error. Presently, $h$ may be measured to an accuracy of 1 µm, which represents an error of 0.01% for a 10-mm thick sample.

The errors in time are caused by the lack of synchronization between VISAR signals and by the time resolution, $dt$, of the VISARs. After synchronization of the data there remains a possible systematic error of up to ±½ $dt$ between channels. This error can have a significant effect on the accuracy of $C_L$. For example, for $h$ = 1 mm, $C_L$ = 7 km/s, and $\Delta t$ = 143.86 ns, an error of ±1/2 ns would render an error in $C_L$ of up to ± 0.35%.

Despite these systematic timing errors, for the results to be consistent they must all lie on the same isentrope. Consequently, the data may be adjusted by a minimization algorithm that adds a fixed time correction to each curve in turn until the standard deviation between the $C_L$ vs. stress curves is minimized and the data are self-consistent;

**Table 1**. Relative errors in ICE experiments.

| Error | HEPP-ICE error |
|---|---|
| B-field non-uniformity across sample, a few % | ≤ 0.1% |
| B-field sample-to-sample non-uniformity, a few % | Zero |
| Thickness: ±0.1% for 1-mm | ±0.01% |
| VISAR timing: for 1-mm at 10 km/s = ±0.1%, ±0.5% | ±0.01%, ±0.05% |
| VISAR velocity ±0.1% to ~2% | Same |

these adjustments must lie within ±½ *dt*. This algorithm works well but presently lacks mathematical rigor. However, using this algorithm the standard deviation between records was reduced to ~0.2% for the copper data. These data demonstrate the capabilities of the technique, but until we can devise a rigorous algorithm we cannot assert that 0.2% is the true error. The use of a velocimeter (VISAR or PDV [16]) with better time resolution is preferred. All errors are summarized in Table 1.

# IV. SUMMARY

It has been shown that the HEPP-ICE load configuration can produce magnetic stress uniformity to better than 1 part in 1000 over the central 87% of the sample faces, and it provides exact matching of the stresses between opposing samples. A large-scale HEPP-ICE system is capable of producing shock-free loading up to 2.2 TPa in 10 mm thick tungsten samples.

The accuracy of the HEPP-ICE system is enhanced by the uniformity and matching of magnetic stress loading, and by the larger sample sizes that can used in HEPP-ICE. Data for tungsten (and copper) have been presented which demonstrate the inaccuracies of the technique, which may be as low as 0.2% in stress.

# V. ACKNOWLEDGEMENT

The authors wish to acknowledge Dennis Herrera, Ross Meyer and Dave Torres for their superb experimental work. This study depended heavily on the excellence of the VISAR team, namely: Paulo Rigg, Darcie Dennis-Koeller, Brian Jensen, Frank Abeyta and Max Winkler. The authors wish to acknowledge Ross Meyer for his outstanding hardware design and manufacturing support.

# VI. REFERENCES

[1] D.G. Tasker, "Isentropic Compression Experiments Using High Explosive Pulsed Power," in Proc. The Ninth International Conference On Megagauss Magnetic Field Generation And Related Topics, Megagauss IX, July 2002, Russia, pp. 765-771.

[2] D.G. Tasker, "Equation of State Experiments in Extreme Magnetic Fields," in Megagauss X, July 2004, Berlin, pp. 211-217.

[3] D.G. Tasker, "Summary of Isentropic Compression Experiments Performed With High Explosive Pulsed Power," presented at Megagauss XI, Sept 2006, London.

[4] J.R Asay, "Isentropic Compression Experiments on the Z Accelerator," American Physical Society, Shock Compression of Condensed Matter (SCCM) (1999), p.261.

[5] J.-P. Davis et al., "Magnetically driven isentropic compression to multimegabar pressures using shaped current pulses on the Z accelerator," Physics of Plasmas **12**, 056310 (2005).

[6] D.B. Reisman, "Magnetically driven Isentropic Compression Experiments on the Z Accelerator," JAP, 89(3), p.1625, 1 Feb. 2001.

[7] D.B. Reisman, "Isentropic Compression of LX-04 on the Z Accelerator," SCCM (2001), p. 849.

[8] J.B. Aidun and Y.M. Gupta, JAP, **69**, 6998 (1991).

[9] D.G. Tasker, et al., "High Current, Low Jitter, Explosive Closing Switches," in Proc. IEEE Pulsed Power Conference, 2003, Monterey, CA, USA, p.517.

[10] J.H. Goforth, "Design of High Explosive Pulsed Power Systems for 20 Mb Isentropic Compression Experiments," in Proc. Megagauss IX, July 2002, Russia, pp. 137-147.

[11] D.G. Tasker, "Equation of State Experiments in Extreme Magnetic Fields," in Proc. Megagauss X, July 2004, Berlin, pp. 211-217.

[12] FlexPDE Professional, Version 5.0.16, PDE Solutions Inc, P.O. Box 609, Sunol, CA , 94586

[13] F.H. Harlow and A.A. Amsden, "Fluid Dynamics, A LASL Monograph," Chapter III, LA-4700, June 1971, Los Alamos Scientific Laboratory, University of California, Los Alamos, New Mexico, 87544.

[14] D.B. Hayes, "Backward Integration of the Equations of Motion …," Sandia National Labs., SAND2001-1440, May 2001.

[15] L.M. Barker and R.E. Hollenbach, "Laser Interferometer for Measuring High Velocities of any Reflecting Surface," JAP, 43, pp.4669-4675 (1972).

[16] O.T. Strand, D. R. Goosman, C. Martinez, T. L. Whitworth, and W. W. Kuhlow, "Compact system for high-speed velocimetry using heterodyne techniques," Review of Scientific Instruments, 77, 083108 (2006)